



Upper Air Humidity from Automatic Aircraft Surveillance Data

Siebren de Haan¹

¹KNMI, De Bilt, the Netherlands

Correspondence: Siebren de Haan (Siebren.de.Haan@knmi.nl)

Abstract. Upper air humidity information is under sampled in the current operational meteorological observing network. Radiosondes observations form the backbone, but radiosondes balloons are typically launched only once or twice per day to limit the costs. The number of aircraft humidity observations are low in Europe, because in Europe only a few aircraft are equipped with water vapour sensors.

- 5 In this paper a novel technique is presented to derive humidity information from aircraft Automatic Dependent Surveillance Broadcast (ADS-B) data, whenever an aircraft is descending or ascending. The retrieved virtual temperatures observations, averaged over a vertical layer of 500 m, have an accuracy between 0.5 K and 0.75 K when compared to European Centre for Medium Range Forecast (ECMWF). Using additional external temperature information, estimates of the specific humidity can be calculated
- 10 with an accuracy of 3-4 g kg⁻¹ and in some cases between 2-3 g kg⁻¹ (that is, when more than 20 estimates are available at the same reference height within 20 minutes). Applying the method to measurements from the Falcon F20 French research aircraft SAFIRE shows that even a single aircraft can be used to derive high-quality virtual temperature information (observation error \approx 0.5 K). Comparison with Aircraft Meteorological Data Relay (AMDAR) and radiosonde humidity showed similar statistics.
- 15 Since ADS-B data is received from all ascending or descending aircraft in the vicinity of an airport, a vast amount of upper air virtual temperatures could be made available, when ADS-B information is gathered by ADS-B receivers installed at, or nearby airports.



1 Introduction

20 Humidity plays a key role in meteorology as it is the driving force for exchange and transport of energy through vaporization and condensation. Despite its significant importance, humidity is under sampled in the current observing system used for operational meteorology.

At present, in-situ observations from balloon (or radio) soundings and selected (commercial) aircraft are the only source of upper air humidity available for making, for example, short range weather forecasts, but the coverage in space and time of these observations is coarse. Radio soundings are launched typically once or twice per day (because radio soundings are costly) while the number of aircraft that measures humidity is small despite aircraft humidity has proven to be valuable (Moninger et al., 2010; Ingleby et al., 2021). Although aircraft data are exploited for (almost) continuous measuring wind and temperature by means of Mode-S Enhanced Surveillance (de Haan et al., 2025), humidity can not be extracted from Mode-S EHS with adequate accuracy (Stone and Kitchen, 2015). Drones equipped with humidity sensors can be a good alternative for radiosondes (Bärfuss et al., 2023), but are not yet fully exploited.

To fill the humidity information gap for Numerical Weather Prediction (NWP) models, humidity information from satellites are used at initial forecast time during the analysis step. Geo-stationary and polar orbiting satellites measure humidity signals by passive sounders and sense radiation emitted from top of atmosphere; humidity signals from lower altitudes are (partially) obscured by overlying humidity or clouds and therefore the uncertainty of humidity information from satellites becomes larger when nearing the surface.

Tropospheric delays from Global Navigation Satellite System (GNSS) contain information of the temperature and humidity along the signal path (Guerova et al., 2016) when a network of GNSS receivers data is processed. GNSS Slant Delays might reveal 3-D water vapor structures when assimilated into a high resolution NWP model (Gutman et al., 2004; Järvinen et al., 2007; Poli et al., 2007; Smith et al., 2007; Bauer et al., 2011; Lindskog et al., 2017).

The above-mentioned humidity observations are either costly (and thus not frequent) or indirect (and thus require some interpretation step) and/or are not accurate and the coverage lack frequent observation in the boundary layer.



This paper shows that height information from aircraft Automatic Dependent Surveillance-Broadcast (ADS-B) data can be exploited to derive virtual temperature and, when an accurate temperature observation is available, a measurement of specific humidity. Moreover, the method could be applied to any ascending or descending aircraft with access to the height information from the board computer.

50 The method presented in this paper exploits the mandatory ADS-B information, transmitted by an aircraft to avoid aircraft collisions. The paper is organized in the following way. First, ADS-B is shortly explained in the next paragraph, which is followed by a description of the algorithm used in this paper to extract humidity information. In the fourth paragraph, measurements from the French atmospheric research aircraft show that this algorithm is capable of retrieving accurate virtual temperature, accurate
55 enough to estimate specific humidity with an error around 2-3 g kg⁻¹. Also shown in this paragraph, are comparison of ADS-B humidity information against NWP model data from the European Centre Medium Weather Forecasts model, AMDAR Humidity and radiosondes. Averaging humidity estimates of multiple aircraft results in accurate ADS-B humidity observation. The last paragraph contains the conclusions and recommendations.

60 2 ADS-B humidity from general air traffic information

ADS-B allows an aircraft to broadcast continuously its position and its intentions primarily for flight safety purposes. The ADS-B system has proven to be an essential element for flight safety. Aircraft, and in some cases other airborne carriers such as gliders or hot-air balloons, are nowadays obliged to carry an active transponder.

65 Information on position and height is autonomously broadcast about every 0.5 seconds and contains the aircraft's onboard sensed position (through GPS and inertial systems). Figure 1 gives an example of the coverage of the data used in this study, also show are the locations of the airports and radiosonde launch sites used later.

2.1 ADS-B height information

70 An ADS-B transponder continuously broadcasts messages which contain position and pressure altitude and GNSS altitude. All height information is truncated to 25 ft (approximately 7.62 m). The pressure

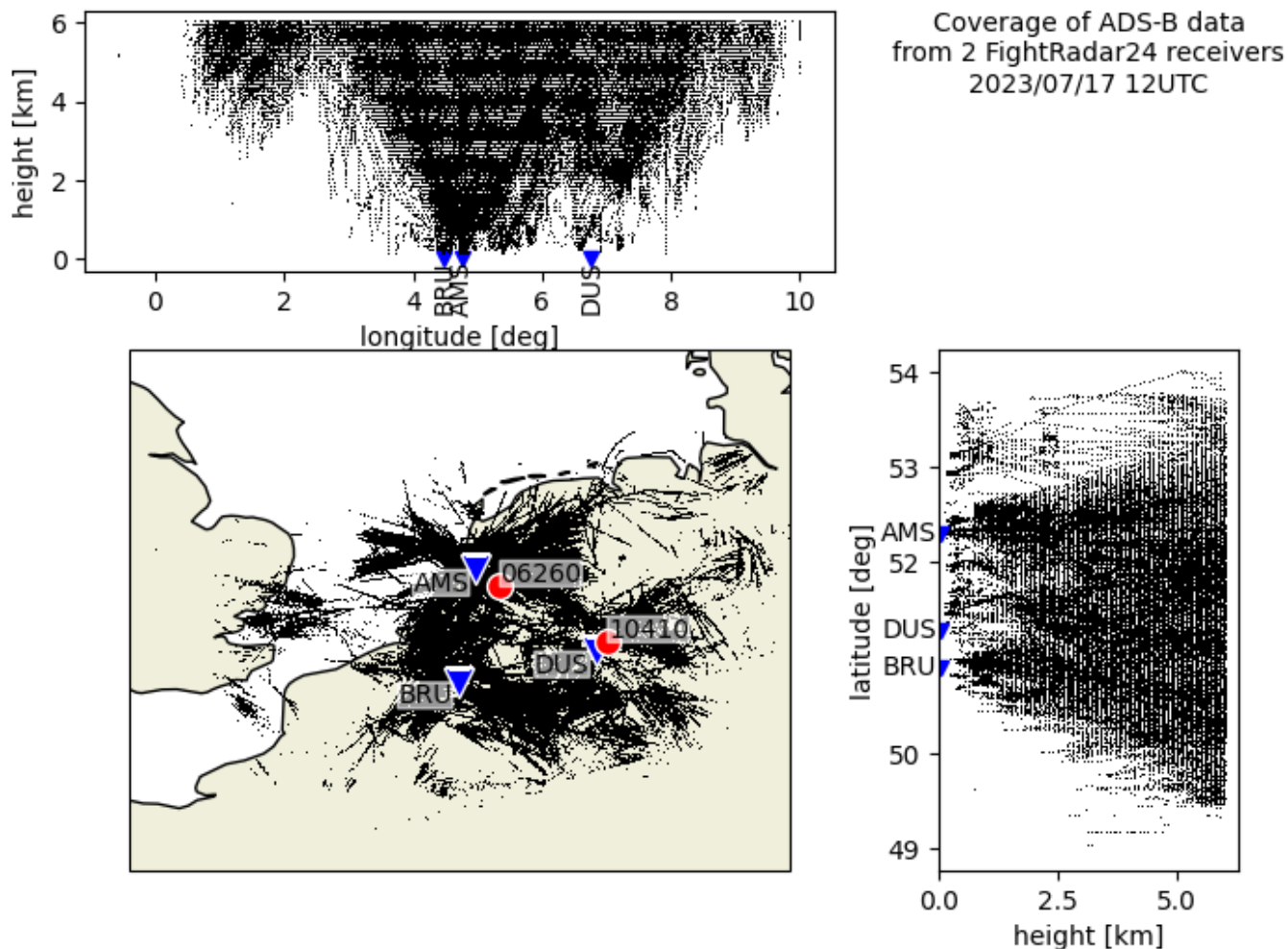


Figure 1. Example of coverage of ADS-B data. Also shown are the radiosonde launch locations (red circles, wmoid’s 06260 and 10410) and three major airports (Amsterdam, Brussel and Düsseldorf).

altitude is broadcasted twice per second, while geometric height information is generally broadcasted with a lower update frequency (up to once per 4 seconds).

All aircraft broadcast pressure altitude and geometric height, and thus an enormous amount of data will be available in busy airspace, like Amsterdam and London.



3 Methodology to derive virtual temperatures

3.1 Virtual temperature

Pressure altitude and geometric height are two different notions of the vertical coordinate in the atmosphere. Geometric height h is the height in meters as can be measured by the GNSS system. Pressure altitude H is the height (generally in feet) according to the international standard atmosphere (ISA) which has prescribed temperature profile and is assumed to be dry and in hydrostatic balance. The temperature profile follows a constant lapse rate of $\beta_0 = -6.5 \text{ K km}^{-1}$, with a temperature of 288.15 K at mean sea level $p_0 = 1013.25 \text{ hPa}$. The pressure altitude is calculated from the surface (p_0) to given pressure value p , as

$$85 \quad H(p) = \int_{p_0}^p \frac{R_d T_{isa}}{g_0} d \log p = \frac{T_0}{\beta_0} \left(1 - \left(\frac{p}{p_0} \right)^{\frac{\beta_0 R_d}{g_0}} \right), \quad (1)$$

with $R_d = 287.0528 \text{ [J K}^{-1} \text{ kg}^{-1}]$ is the specific gas constant for a dry air, and $T_{isa} = T_0 - \beta_0 H$

The geometric height h of an aircraft flying at pressure level p depends on the temperature and humidity profile from the surface p_0 up to the pressure p ,

$$h(p) = \int_{p_0}^p \frac{RT}{g} d \log p, \quad (2)$$

90 where R is the universal gas constant (depending on the composition of the volume of air, i.e. humidity), g is the gravitational acceleration, where it is assumed that the air is in hydrostatic equilibrium and ideal gas law is applicable. Writing the geometric height as a function of pressure altitude and calculating the derivative to H gives

$$h(H) = \int_{H_0}^H \frac{RT}{R_d T_{isa}} \frac{g_0}{g} dH \Leftrightarrow \frac{dh}{dH} = \frac{g_0}{g(h)} \frac{RT}{R_d T_{isa}}. \quad (3)$$



95 It is common to express $RT = R_d T_v = R_d T(1 + \delta q)$ with $\delta = 0.608$ [-], and q specific humidity [g kg^{-1}]. Then the virtual temperature can be found by

$$T_v = \frac{dh}{dH} \frac{g(h)}{g_0} T_{isa}. \quad (4)$$

3.2 Algorithm

The derivate of h to H is the partial (or local) derivative. It can be computed from the total time derivates
100 of H and the difference between geometric height and pressure altitude $G = h - H$, assuming that the pressure related terms can be neglected for G . This results in

$$\frac{\partial h}{\partial H} = \left(\frac{dG}{dt} \right) \left(\frac{dH}{dt} + \nabla \cdot \Phi_h \right)^{-1} + 1, \quad (5)$$

where Φ_h is geodetic height as defined by Lemoine et al. (1998). Estimates of derivatives are determined using central three point approximation for observations during ascends and descends (i.e. parts of the
105 flight where values of H_i decrease or increase monotonically). The following steps are performed to estimate virtual temperature:

1. *Preparation*: Prepare time series and select ascending and descending phase. Remove outliers and measurements with large roll angle¹,
2. *Averaging*: The height measurement from aircraft have some kind of error. Because observed ADS-
110 B values are truncated during data exchange, these observations are not accurate enough. The values of H and h will be change with time, averaging over a time window (or vertical bin) will reduce the truncation error. This is more or less equivalent to applying a low pass filter;
3. *Estimating*: Calculate the approximate value of $\partial h / \partial H$ for a number of different incremental steps with associated average and standard deviation;

¹Please note that roll angle is not contained in the ADS-B messages; here roll angle information from Mode-S EHS BDS-50 is merged. In Europe responds to BDS-50 interrogation is obligatory. When roll angle information is not available, a quality measure could be inferred from for example the flight path.



115 4. *Selecting*: Measurements found in (nearly) the same 4D flight paths, and the same destination or airport of departure, are combined; selection is based on number of valid virtual temperatures and standard deviations of estimates.

3.3 Humidity information and errors

Virtual temperature is a function of temperature and humidity and to separate humidity additional temperature information is necessary. This implies that the accuracy of the humidity information depends on the accuracy of the virtual temperature as well as on the temperature accuracy. When ADS-B height data is combined with an external temperature source, the errors of virtual temperature and temperature will be independent and the error in estimated specific humidity q will be the sum of virtual temperature error and temperature error, because

$$125 \quad q = \frac{1}{\delta} \left(\frac{T_v}{T} - 1 \right).$$

The error in q when derived from virtual temperature can be approximated by, using Taylor (1997)

$$\sigma_q^2 \approx \left(\frac{\partial q}{\partial T} \right)^2 \sigma_T^2 + \left(\frac{\partial q}{\partial T_v} \right)^2 \sigma_{T_v}^2 \approx \frac{2}{\delta T^2} \sigma_T^2.$$

Note that the error is inversely related to the temperature, for example a measurement of q at a temperature of 288.15 K (15 °C) with an error of 1 K will have an error around 8 g kg⁻¹. So to derive q from virtual temperature with some skill (i.e. with an error of around 3-4 g kg⁻¹) an accurate temperature measurement is required ($\sigma_T \approx 0.4 - 0.5$ K); the skill of the estimate of q will decrease for decreasing temperatures (i.e. increasing height).

The error in the estimated virtual temperature is related to the accuracy of the estimated derivative of h to H , approximated by

$$135 \quad T_v \approx \left(\frac{\Delta h}{\Delta H} \right) (T_0 - \beta_0 H). \quad (6)$$

The error in the absolute height estimate can be as large as 7 meter, however the underlying errors (i.e. GNSS satellite clock errors) can be assumed constant over a short epoch, and will therefor cancel, resulting



in an accurate height change measurement. The variance of ΔH is twice the variance of H , and applying again Taylors approximation, an estimate of the error becomes

$$140 \quad \sigma_{T_v}^2 \approx \left(\frac{\overline{T_0 - \beta_0 \overline{H}}}{\Delta H} \right)^2 \sigma_{\Delta h}^2 + \left(\frac{\overline{\Delta h T_0 - \beta_0 \overline{H}}}{\Delta H^2} \right)^2 \sigma_{\Delta H}^2 + \left(\beta_0 \frac{\Delta h}{\Delta H} \right)^2 \sigma_H^2 \quad (7)$$

The \overline{H} denotes the average value of measurements of H over the dataset at hand. For layer depths of 200-500 m and because $\Delta h \approx \Delta H$ the estimate becomes (neglecting the last term)

$$\sigma_{T_v}^2 \approx \frac{T_0}{\Delta H} (2\sigma_h^2 + 2\sigma_H^2). \quad (8)$$

Note that T_0 puts restrictions on the choice of ΔH , that is a $\Delta H \ll T_0$ will have a large error.

145 4 Results

This section contains the results of the estimation of virtual temperature from real aircraft observations. First, observations obtained by several campaigns performed by the French atmospheric research aircraft Falcon F20 is used to show the proof of concept. Data from this aircraft contained all necessary information (time, height, position, pressure altitude and humidity). Next the algorithm is applied to actual
150 transponder data made available through the UK MetOffice Global EHS project for a two-month period. The results are compared to ECMWF model equivalents, AMDAR-humidity and radiosondes observations.

4.1 Proof of concept using research aircraft data

The French Falcon F20 atmospheric research aircraft has made several flights in French airspace for
155 special campaigns (e.g. validation of satellite retrievals). The aircraft was equipped with laser-diode based Water Vapor Sensing System (WVSS-II) which can measure the amount of water vapour very accurately. Together with high resolution GNSS height and pressure observations conducted at 1 Hz this opens the possibility to test the previously described algorithm. Height measurements are binned in the vertical to improve on the accuracy, especially because the ADS-B height information is truncated.

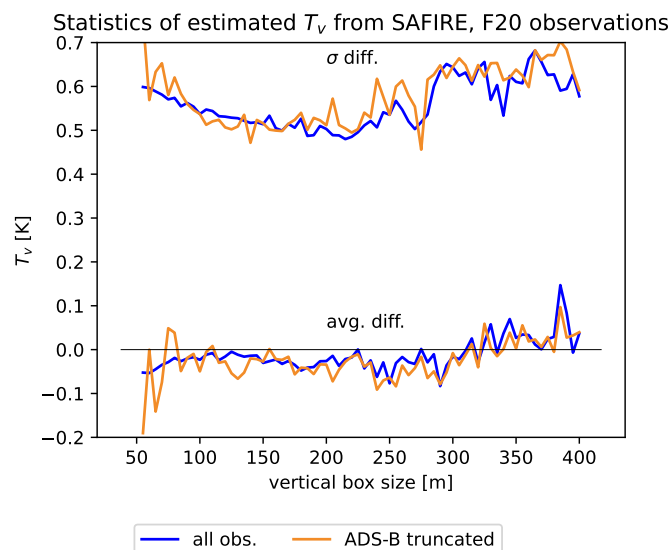


Figure 2. Statistics of virtual temperature estimation from height observations measured by SAFIRE Falcon F20 with respect to different vertical box sizes. Two solutions are shown: in blue denotes the solution based on the full resolution of the height information. The orange lines are the estimates when the heights were truncated with 25 ft. The bottom two lines express the average difference of the solution and observation; the standard deviation are the top two lines. Aircraft data from 17 days (between 2019/09/16 and 2021/09/19) were used (Richard, 2019).

160 Figure 2 presents the results of estimating and measuring virtual temperature using data from measurement campaigns performed by the research aircraft of Meteo-France (Richard, 2019). The average of the difference is close to zero and the standard deviation has a minimum value of approximately 0.5 K. The noisy character of the blue lines is due to the limited number of data points. The orange lines in Figure 2 are the estimates determined after an ADS-B truncation is applied to the measured geometric height and
165 pressure altitude. The effect of truncation is mainly visible as some extra noise.

A reasonable choice for the vertical box size is around 150 m; the standard deviation with WVSS-II measurements is around 0.5 K which implies that, given an accurate temperature, the specific humidity could be constructed with acceptable error characteristics.

4.2 Results from two months of ADS-B observations

170 Live recorded ADS-B information was obtained for a two-month summer period. The summer was chosen because virtual temperature is measured more easily at temperatures above 0 °C. The ADS-B data has been

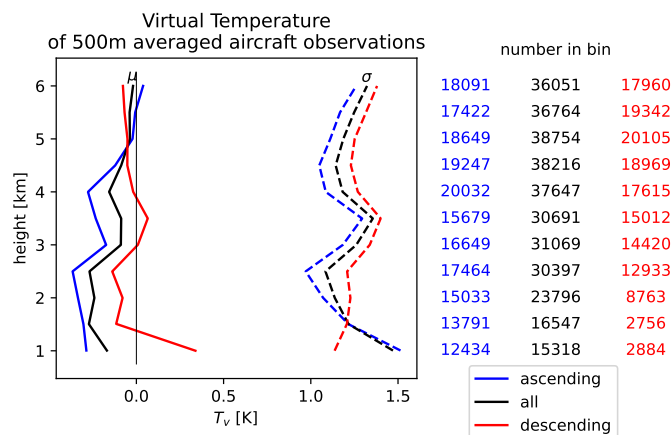


Figure 3. Statistics of virtual temperature comparison against ECMWF equivalents, averaged over 500 m, along individual flight paths, starting or ending at Amsterdam Schiphol Airport. Each vertical box contained on average at least 5 ADS-B observations (and at most 7). The average difference (solid lines) and standard deviation of difference (dashed lines) are shown for ascending (blue), descending (red) and both flight phases (black). Data is gathered for the period 2023/07/06 to 2023/08/31.

collected by FlightRadar24 and was delivered to KNMI within the Global-Mode-S EHS project from the UK MetOffice. Special care has been taken to decode the position information from the even/uneven position messages.

175 4.2.1 Comparing ADS-B humidity against ECMWF

The virtual temperature estimates from (averaged) aircraft are compared to ECMWF equivalents. Temperature observations (and roll angle information) from the EMADDC-processing (de Haan et al., 2025) chain were merged into the dataset and virtual temperatures were estimated by the algorithm described previously. These raw virtual temperature estimates have standard deviation of around 1.8 K (not shown) when compared to ECMWF, which is too noisy for use in NWP. To achieve better quality, observations falling in the same 20-minute window, from each aircraft, are averaged over 500 m bins. Since ascending and descending flight paths differ from each other in space and time, both flight phases are treated separately. The resulting virtual temperatures are less noisy with a standard deviation between 1 and 1.5 K, when compared to ECMWF virtual temperatures. Figure 3 shows the statistics for virtual temperature, averaged over its flight path every 500m, compared to ECMWF. The virtual temperature has a small bias (in



mostly negative around -0.25 K to -0.35 K for ascending aircraft and around zero for descending aircraft). The signature for ascending aircraft is remarkable. The bias changes with height; this could well be related to changing of aircraft flight phase (e.g. change in airspeed, extra flaps, or landing gear for descending, and pitch for ascending). The quality of derived specific humidity (i.e. retrieved from temperature and virtual temperature, both with an error of 1 to 1.5 K) is not good enough to estimate the relative humidity with some kind of skill. The virtual temperature itself, could be valuable for assimilation in NWP.

Observations of virtual temperature with better quality were found when estimates from all aircraft close in space and time are averaged, creating super-observations. These observations were created from aircraft which were landing (or departing) at/from the same airport/runway. Averages of virtual temperature were determined for observations that are in the same 500 m vertical box with observation times falling in the same 20-minute interval. The statistics are depicted in Figure 4, which shows temperature, virtual temperature and specific and relative humidity of ADS-B derived estimates compared to ECMWF equivalents. The standard deviation of virtual temperature improves to error values just above 0.5 K. The error reduction in both temperatures reduces the error in specific humidity and consequently the relative humidity estimate. The error in relative humidity now becomes around 50 %. The biases of virtual temperature, specific humidity, and relative humidity is small, but exhibit a linear trend with height. Note furthermore that the bias in (EMADDC) temperature becomes positive for low heights. This is an artifact of the Mode-S EHS processing and will be addressed in future research.

The amount of observations remaining when observations averaged over less 20 observations are removed, is shown in Figure 5. Clearly before 5 UTC and after 23 UTC the number of aircraft landing/departing is too low, but for the other times the distribution with height looks good, with an emphasis on heights around 2 km and above 5 km. Especially the number of observations around 2 km are expected to be valuable, when temperatures are above zero.

4.2.2 Comparing against AMDAR-humidity and radiosonde

A (small) number of AMDAR aircraft are equipped with a WVSS-II water vapour sensor, and were present in the Dutch airspace during the period of interest. These aircraft were collocated with (other) ADS-B aircraft to compare the virtual temperature. Except the water vapour sensor carrier, all ADS-B observations were used for comparison. The resulting statistics are show in Table 1, showing only



Observation averaged per airport per 500m vertical bin and 20' window
 Period 2023-07-06 - 2023-08-31

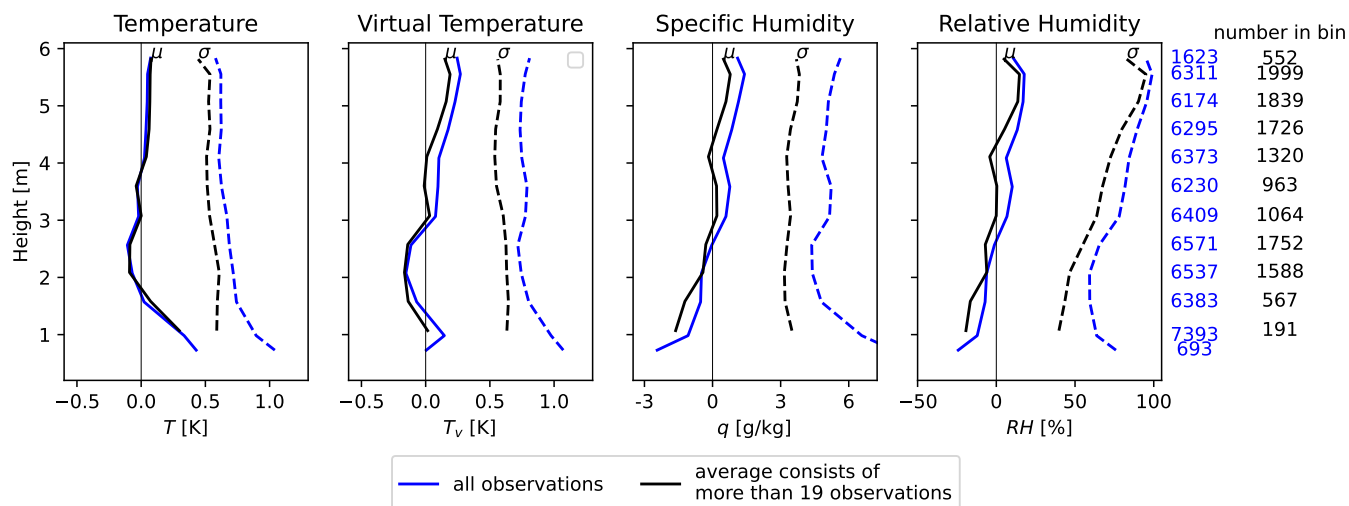


Figure 4. Estimation of virtual temperature averaged over 500m, along combined flight paths which are within 20 minutes, starting or ending at Amsterdam Schiphol airport. On average each vertical box contained 5 or more different aircraft. Comparison is against ECMWF equivalent. Note that the temperature is obtained from EMADDC-processing and is used to calculate *RH* together with a pressure measurement.

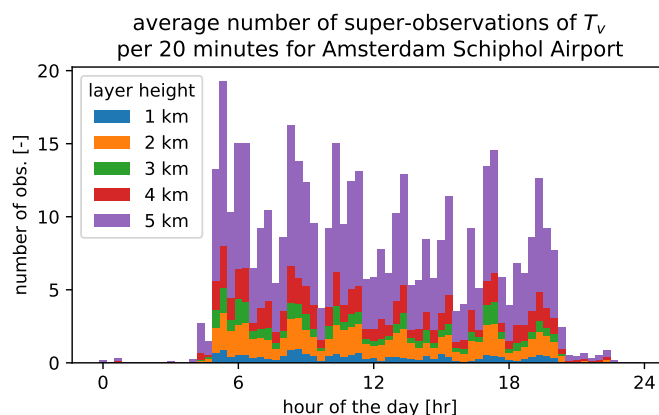


Figure 5. Average number of super-observations per 20 minutes per kilometer height. Super-observations are average values of a set of equal or more than 20 T_v observations.

33 collocations of AMDAR-humidity with ADS-B virtual temperatures. The reason is that most of the
 215 AMDAR-humidity aircraft in the vicinity of the Dutch airspace are flying between British and German
 airports, and thus the number of profiles at Amsterdam airport is small.



Table 1. Statistics of collocated ADS-B with AMDAR and radiosonde observations (RS). Both AMDAR and RS observations are compared to airport/runway averages. An ADS-B observation is collocated when the distance was smaller than 50 km and the time difference was smaller than 30 minutes to the other platform observation. Temperature and humidity observations from radiosonde and AMDAR were interpolated to the same height as the ADS-B observation.

platform	number	$T_v^{adsb} - T_v^{pl}$ [K]		$T_v^{adsb} - T_v^{nwp}$ [K]		$q^{adsb} - q^{pl}$ [g kg ⁻¹]	
		μ	σ	μ	σ	μ	σ
AMDAR	33	-0.39	0.78	0.10	0.81	-2.38	2.18
RS	53	-0.06	0.75	-	-	0.94	2.37

The dataset used for the AMDAR and RS comparison was the averaged airport/runway data, with super-observations averaged over all observations (blue line in Figure 4). Collocated ADS-B and AMDAR observations were found when the distance was less than 50 km, and the time difference was less than 30 minutes. The 33 collocated observations have a standard deviation of 0.78 K which is in accordance with Figure 4. The standard deviation of the specific humidity of around 2 g kg⁻¹ is small however the bias is of the same order, so no solid conclusions can be drawn with respect to the specific humidity.

Also shown in this table are the statistics of collocated ADS-B and radiosonde observations. The number of collocations is (again) small because there are not many radiosonde launches in the area of interest, and they were performed mainly at 00 UTC, at which time there are only sporadic aircraft landing or departing (see Figure 5).

The 53 radiosonde observations are compared to the averaged airport data. Figure 6 shows all radiosonde observations that are collocated with radiosonde De Bilt, the Netherlands (14 times, WMO-id 06260) with EHAM (Amsterdam Schiphol Airport) and one time Essen, Germany (WMO-id 10410) with EDDL (Düsseldorf, Germany) observations. The distance between both observations is at least 35km, which adds some extra uncertainty to the comparison. In some cases, the observed humidity appears to be an outlier (e.g. 2023/07/21 00UTC), while other cases the observations are coherent in time (not shown, 2023/08/10 12UTC) and thus the actual profiles may differ substantially. A longer period of comparison could reveal systematic differences, nevertheless the ADS-B observations are on average inline with the radiosonde profile.

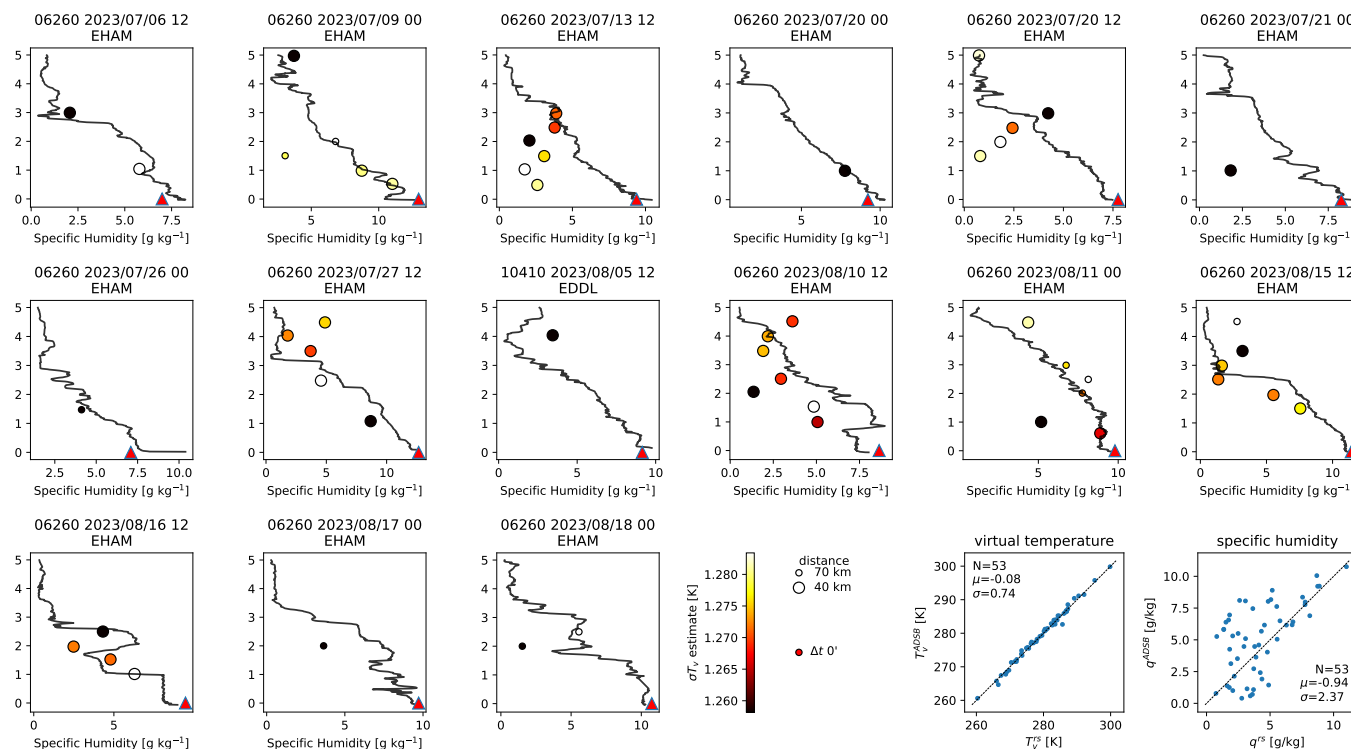


Figure 6. Profile comparison of all 53 observations from ADS-B over the period from 2023/07/06 - 2023/08/31. The sample standard deviation of T_v is represented by the color scale. The size of the circle relates to the distance between radiosonde observation and ADS-B observation, and the standard deviation of the estimated virtual temperature. The last two panels in the lower right corner show the scatter plots of virtual temperature and specific humidity. The red triangle denotes the surface specific humidity.

5 Summary, Conclusions and Recommendations

A new method was developed to extract humidity information from high frequency aircraft height information. The obtained estimates of virtual temperature appears to be bias free and with standard deviation around 0.75 K when compared to in-situ observations from an atmospheric research aircraft. These values are encouraging and lead to an accurate specific humidity observation with an error of about 3-4 g kg^{-1} . Note that the presented algorithm is rather basic and can be improved in several ways to filter and estimate the derivative more accurately. A possible candidate algorithm could be the Savitzky-Golay method, which allows for proper estimation of derivatives (Savitzky and Golay, 1964).



The study with data from research aircraft showed that this method has potential for operational use
245 and could be used to measure upper air humidity. Furthermore, this algorithm could be added to existing
software that already generates observations for meteorology, on board an aircraft (for example AMDAR
software) to measure virtual temperature continuously when an aircraft is descending or ascending.

This paper also showed that ADS-B data can be exploited to estimate virtual temperature when aircraft
are changing height. When deployed to data from a busy airport like Amsterdam Airport Schiphol the
250 time and space averaged data (500 m in the vertical and 20 minutes) is of good quality when compared to
NWP. The observations have a mean error which is close to zero and standard deviation between 0.5 and
0.75 K. These observations satisfied the minimum requirement for derivation of specific humidity with
adequate quality.

Comparison of ADS-B observations based on aircraft movements at Schiphol airport with radiosonde
255 and AMDAR observations are in agreement with earlier found statistical values when comparing to
ECMWF, albeit that the number of collocations with both radiosonde and AMDAR are small.

Given the observations with presented uncertainties a positive impact on short range forecast of upper
air humidity is envisaged when these observations are assimilated.

5.1 Conclusions

260 The following can be concluded

1. High quality virtual temperatures can be obtained by observations of the change of geometric heights
with respect to pressure altitude,
2. The algorithm developed can be applied to ADS-B data and for a busy airport good quality virtual
temperatures can be obtained (estimated error of the order of 0.5 - 0.75 K),
- 265 3. The very basic algorithm can be enhanced for better estimates,
4. Because ADS-B is the input, this algorithm can be applied globally.



5.2 Recommendations

1. Running a trail with live or off-line height observations over a long period (one year) should prove the quality of this information.
- 270 2. The impact of virtual temperature assimilation on short range weather forecast on air humidity should be investigated and especially the combined use of ADS-B virtual temperatures and other humidity related observations (GNSS, MTG-IRS, and even ceilometers) should be exploited. The ADS-B derived virtual temperatures are mainly available from 5 UTC to 21 UTC but combined with other observations this will lead to a better constraint NWP initialization.
- 275 3. It might be considered to adapt AMDAR software (if possible) to estimate virtual temperature. As a first attempt, high temporal observations from research aircraft could be exploited in a real time setting for further proof.

Data availability. Data used from the French research aircraft was obtained using the CEDA portal (<http://ceda.ac.uk>); The ADS-B data was provided by FlightRadar24 obtained within "The global Mode-S EHS" project, through an
280 agreement between the UK MetOffice and KNMI. The Mode-S EHS temperatures were extracted from the KNMI data platform (<http://datapatform.knmi.nl>)

Competing interests. There is no competing interests present

Acknowledgements. The author acknowledges the use of (raw) ADS-B data from FlightRadar24, and the UK Metoffice for initiating and running the Global Mode-S EHS project. The crew, technicians and researchers from
285 MetoeFrance are acknowledgements for making the trials and making the data available. The CEDA database is thanked for easy disclosure of the data. Part of the work is done within the KNMI EMADDC program, which is co-financed (2016-2024) by the Connecting Europe Facility of the European Union.



References

- 290 Bärffuss, K. B., Schmithüsen, H., and Lampert, A.: Drone-based meteorological observations up to the tropopause – a concept study, *Atmospheric Measurement Techniques*, 16, 3739–3765, <https://doi.org/10.5194/amt-16-3739-2023>, 2023.
- Bauer, H.-S., Wulfmeyer, V., Schwitalla, T., Zus, F., and Grzeschik, M.: Operational Assimilation of GPS Slant Path Delay Measurements into the MM5 4DVAR System, *Tellus A*, 63, 2011.
- de Haan, S., de Jong, P., Koutek, M., Sondij, J., and Strauss, L.: EMADDC: high-volume, high-quality, and timely
295 wind and temperature observations from aircraft surveillance data (Mode-S EHS), *Atmospheric Measurement Techniques*, 18, 3341–3359, <https://doi.org/10.5194/amt-18-3341-2025>, 2025.
- Guerova, G., Jones, J., Douša, J., Dick, G., de Haan, S., Pottiaux, E., Bock, O., Pacione, R., Elgered, G., Vedel, H., and Bender, M.: Review of the state of the art and future prospects of the ground-based GNSS meteorology in Europe, *Atmospheric Measurement Techniques*, 9, 5385–5406, <https://doi.org/10.5194/amt-9-5385-2016>, 2016.
- 300 Gutman, S. I., Sahm, S. R., Benjamin, S. G., Schwartz, B. E., Holub, K. L., Stewart, J. Q., and Smith, T. L.: Rapid Retrieval and Assimilation of Ground Based GPS Precipitable Water Observations at the NOAA Forecast Systems Laboratory: Impact on Weather Forecasts, *J. Met. Soc. Japan*, 82, 351–360, 2004.
- Ingleby, B., Candy, B., Eyre, J., Haiden, T., Hill, C., Isaksen, L., Kleist, D., Smith, F., Steinle, P., Taylor, S., Tennant, W., and Tingwell, C.: The Impact of COVID-19 on Weather Forecasts: A Balanced View, *Geophysical Research
305 Letters*, 48, e2020GL090699, <https://doi.org/10.1029/2020GL090699>, 2021.
- Järvinen, H., Eresmaa, R., Vedel, H., Salonen, K., Niemelä, S., and de Vries, J.: A Variational Data Assimilation System for Ground-Based GPS Slant Delays, *Q. J. Roy. Met. Soc.*, 133, 969–980, 2007.
- Lemoine, F. G., Kenyon, S., Factor, J. K., Trimmer, R. G., Pavlis, N. K., Chinn, D. S., Cox, . M., Klosko, S. M., Luthcke, S. B., Torrence, M. H., Wang, Y. M., illiamson, R. G., C., P., Rapp, R. H., and Olson, T. R.: The
310 Development of the Joint NASA GSFC and the National Imagery and Mapping Agency (NIMA) Geopotential Model EGM96., Tech. Rep. NASA/TP-1998-206861, NASA, 1998.
- Lindskog, M., Ridal, M., Thorsteinsson, S., and Ning, T.: Data assimilation of GNSS Zenith Total Delays from a Nordic processing centre, *Atmospheric Chemistry and Physics Discussions*, pp. 1–22, <https://doi.org/10.5194/acp-2017-567>, 2017.
- 315 Moninger, W. R., Benjamin, S. G., Jamison, B. D., Schlatter, T. W., Smith, T. L., and Szoke, E. J.: Evaluation of Regional Aircraft Observations Using TAMDAR, *Weather and Forecasting*, 25, 627–645, 2010.



- Poli, P., Moll, P., Rabier, F., Desroziers, G., Chapnik, B., Berre, L., Healy, S. B., Andersson, E., and Guelai, F.-Z. E.: Forecast Impact Studies of Zenith Total Delay Data from European near Real-Time GPS Stations in Météo France 4DVAR, *J. Geophys. Res.*, 112, 1–16, 2007.
- 320 Richard, P.: AEOLUS, 2019.
- Savitzky, A. and Golay, M.: Smoothing and Differentiation of Data by Simplified Least Squares Procedures, *Analytical Chemistry*, 8, 1964.
- Smith, T. L., Gutman, S. I., and Sahm, S. R.: Forecast Impact from Assimilation of GPS IPW Observations into the Rapid Update Cycle, *Mon. Wea. Rev.*, 135, 2914–2930, 2007.
- 325 Stone, E. K. and Kitchen, M.: Introducing an Approach for Extracting Temperature from Aircraft GNSS and Pressure Altitude Reports in ADS-B Messages, *Journal of Atmospheric and Oceanic Technology*, 32, 736–743, <https://doi.org/10.1175/JTECH-D-14-00192.1>, 2015.
- Taylor, J. R.: *An Introduction to Error Analysis: The Study of Uncertainties in Physical Measurements*, University Science Books, Sausalito, Calif, 2. ed edn., ISBN 978-0-935702-75-0 978-0-935702-42-2, 1997.